

Evaluation of 1047-nm Photoacoustic Instruments and Photoelectric Aerosol Sensors in Source-Sampling of Black Carbon Aerosol and Particle-Bound PAHs from Gasoline and Diesel Powered Vehicles

W. P. ARNOTT,* B. ZIELINSKA,
C. F. ROGERS, J. SAGEBIEL,
KIHONG PARK, JUDITH CHOW,
HANS MOOSMÜLLER, AND
JOHN G. WATSON

Desert Research Institute, Reno, Nevada

K. KELLY, D. WAGNER, A. SAROFIM, AND
J. LIGHTY

University of Utah, Salt Lake City, Utah

G. PALMER

Hill Air Force Base, Ogden, Utah

A series of measurements have been performed at Hill Air Force Base to evaluate real-time instruments for measurements of black carbon aerosol and particle-bound PAHs emitted from spark and ignition compression vehicles. Vehicles were operated at idle or fast idle in one set of measurements and were placed under load on a dynamometer during the second series. Photoacoustic instruments were developed that operated at a wavelength of 1047 nm where gaseous interference is negligible, although sensitivity to black carbon is good. Compact, efficient, solid-state lasers with direct electronic modulation capabilities are used in these instruments. Black carbon measurements are compared with samples collected on quartz fiber filters that were evaluated using the thermal optical reflectance method. A measure of total particle-bound PAH was provided by photoelectric aerosol sensors (PAS) and is evaluated against a sum of PAH mass concentrations obtained with a filter-denuder combination. The PAS had to be operated with a dilution system held at approximately 150 °C for most of the source sampling to prevent spurious behavior, thus perhaps compromising detection of lighter PAHs. PA and PAS measurements were found to have a high degree of correlation, perhaps suggesting that the PAS can respond to the polycyclic nature of the black carbon aerosol. The PAS to PA ratio for ambient air in Fresno, CA is 3.7 times as large in winter than in summer months, suggesting that the PAS clearly does respond to compounds other than BC when the instrument is used without the heated inlet.

* Corresponding author phone: (775)674-7023; fax: (775)674-7060; e-mail: Pat.Arnott@dri.edu.

Introduction

Quantification of black carbon aerosol is important for both health and the Earth's radiation balance (1, 2), so the accurate, rapid assessment of these aerosols is needed, in both the direct analysis of source emissions as well as in cities or remote locations. Black carbon aerosol is produced by the combustion of fossil fuels and biomass with regional emissions of sufficient magnitude to cause disruptions of atmospheric heating profiles and possibly large-scale perturbations of the Earth's hydrological cycles (3). Historical trends point toward increasing levels of BC production (4). It is unhealthy to breathe the polycyclic aromatic hydrocarbons that may exist in the vapor phase, may be absorbed in liquid-phase aerosol, or may be adsorbed to the surface of black carbon aerosol (5–9). PAHs as a group are reasonably anticipated to be carcinogenic (10), and a few individual PAHs, such as benz[a]anthracene and benzo[a]pyrene, are probably carcinogenic (11). Diesel exhaust has also been linked to allergic inflammation (12) and is considered a probable carcinogen. This paper provides an assessment of real-time instruments for measurement of BC and particle-bound PAHs for use in sampling combustion sources. The source measurements are also contrasted against ambient measurements made at the Fresno, CA Supersite.

The methods for quantifying black carbon mass concentration can be divided into two categories based on whether they require a filter substrate. Examples of filter-based techniques include thermal and optical methods, and laboratory and real-time instruments exist for each. Thermal methods start with the collection of aerosol on a filter, followed by measurement of the carbon atoms evolved when the filter is heated, with elemental carbon being defined as the carbon mass observed in some temperature range. Filter-based optical methods measure the optical attenuation across a filter as aerosols are deposited and exploit the observation that most particulate light absorption in the atmosphere is due to black carbon aerosol. Accurate mass flow meters are vital for quantifying the volume of air sampled to obtain the observed aerosol accumulation on a filter. Filter methods have limitations with respect to dynamic range, lack of a common definition of elemental carbon, and scattering aerosol interferences in the black carbon measurement (13, 14). Photoacoustic instruments are also used to measure BC and they overcome the deficiencies of the filter-based sampling methods (15).

The photoelectric aerosol sensor (PAS) utilizes an ultraviolet lamp to ionize particles containing PAHs. The charged particles are collected on a filter, and the charge is measured with an electrometer. The PAS signal was originally correlated to 17 individual PAHs from several sources, with a universal conversion factor of 1–3 ng m⁻³ femtoamp⁻¹ (16–18). Because PAHs are such a complex mix of vapor and particle-phase compounds, the PAS responds differently to each type of source, and the sensitivity varies in comparison to extractive methods (19). Furthermore, independent evaluations of the PAS are limited, and investigators report widely varying conversion factors (16, 20, 21). A chronicle is provided in this paper of the efforts employed to successfully use the PAS in source sampling, as well as a comparison of results from the PAS with measurements from a filter and denuder sampler followed by extraction and laboratory quantification of individual PAHs. Generally, good correlation is found between BC and PAS measurements raising the following issue: does the PAS respond to the polycyclic nature of the black carbon aerosol? This question takes on particular relevance because the laboratory extractions of PAHs showed

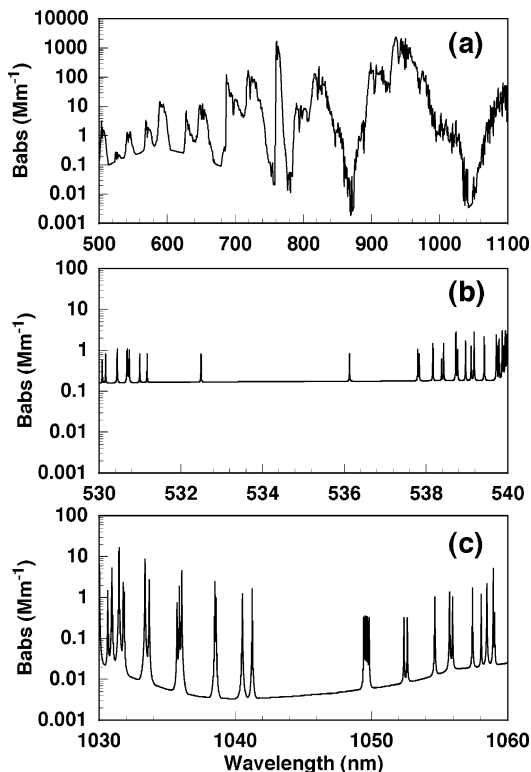


FIGURE 1. Calculation of light absorption by gases in a standard atmosphere for most of the visible and near-IR spectrum (a), and near wavelengths where convenient laser sources are available at 532 nm (b), and 1047 nm (c). Note that gaseous interference is especially low at 1047 nm. The main interfering gas at 532 nm is NO₂, a common gas produced in combustion.

only a weak correlation with BC (5). The tubing inlet for the PAS had to be heated to approximately 150 °C to remove species, perhaps such as unburned oil, that degraded PAS performance, and, in the process, may have also greatly affected the gas-to-particle phase partition.

Photoacoustic Measurements of Aerosol Light Absorption and the Definition of Black Carbon. Photoacoustic instruments have been used in the source sampling of black carbon aerosol. Sample air is pulled continuously through an acoustical resonator and is illuminated by laser light that is periodically modulated at the acoustical resonance frequency. Light absorption is manifested in particle heating and this heat transfers rapidly to the surrounding air, inducing pressure fluctuations that are picked up with a microphone on the resonator. Microphones have a very large dynamic range (at least 6 orders of magnitude), so black carbon measurements can be made over a large dynamic range with these instruments. The advancement that has been very important for the continued success of these instruments is the ability to measure very low levels of light absorption. Aerosol light absorption at visible and near-IR wavelengths occurs throughout the entire particle volume for submicron combustion particles, so black carbon aerosol mass concentration is found to vary in direct proportion with light absorption. Vehicle manufacturers pursued these methods in the 1970s and 1980s using bulky argon ion lasers and dye lasers (22–27), and a resurgence of interest has emerged in research laboratories that coincides with technological developments in compact, efficient laser sources (28–31).

The photoacoustic instrument developed for this work operates at a convenient wavelength of 1047 nm where gaseous interference is not a problem and where a laser source is available that allows for direct electronic modulation of the power at the resonator frequency. Figure 1 shows the

calculated light absorption for a standard atmosphere containing only gases, for it is gaseous interference that could potentially limit black carbon particle detection. Figure 1a shows that a number of microwindows are available where relative minima of gaseous absorption occur. Figure 1b shows the details around a commonly used wavelength of 532 nm. The chief interfering gas at this wavelength is NO₂, giving rise for a need to denude this common combustion gas for practical applications (32). Figure 1c shows that the laser wavelength of 1047 nm is ideal because of the relatively broad range over which gaseous interference is a minimum. NO₂ is not an interferent at 1047 nm, but can be useful in cross-calibrating instruments (33).

The acoustical resonator, shown schematically in Figure 2, was designed for compactness, ease of reproducibility in manufacture, and robustness with respect to use of the instrument in very noisy, dirty sampling environments (34). The instrument comprises two identical coupling sections and a third resonator section, all made of aluminum. The coupling sections allow the laser beam to enter the instrument through windows well separated from the resonator section. The sample inlets and outlets are followed by cavities that are tuned to reduce the coupling of noise into the resonator section. The resonator section has a horizontal tube that is $\frac{1}{2}$ of an acoustic wavelength long, and two vertical tubes that are $\frac{1}{4}$ of an acoustic wavelength long. In previous designs (28), the vertical tubes were at an angle of 45 degrees to the horizontal instead of 90 degrees as they are now, and the tubes were formed from pipe rather than machined with precision. The 90 degree angles allow for symmetry when deciding where the holes in the resonator are placed to allow for laser beam and sample air passage. The piezoelectric transducer is used as a sound source to occasionally scan the resonator resonance frequency and quality factor for use in calibrating the instrument from an acoustical perspective. The microphone and piezoelectric transducer sit at pressure antinodes of the acoustic standing wave. The holes in the resonator for sample and laser beam passage are at pressure nodes where they interfere minimally with the acoustic standing wave. The instrument is bolted together in three parts for easy disassembly in case it needs to be cleaned. The laser beam passes through the windows and the holes in the resonator section. The laser beam pumps the acoustic wave through light absorption, and the associated transfer of heat to the surrounding air, in the resonator section.

The photoacoustic instrument measures the aerosol light absorption coefficient (28, 33), and then a quantity defined as black carbon (BC) is computed from the absorption coefficient. The “elemental” carbon (EC) part of the exhaust absorbs light at 1047 nm much more strongly than any other common particulate aerosol in exhaust and in the atmosphere so that it is reasonable to associate elemental carbon with aerosol light absorption. Aerosol light absorption occurs throughout the entire particle volume for sufficiently small particles and large wavelengths of light, giving rise to a direct proportionality between the absorption measurement and the black carbon aerosol mass for a typical combustion particle and for the 1047-nm wavelength used in the instrument. It is perhaps inevitable to speculate that the aerosol complex refractive index could vary with the combustion source (35, 36) so that the black carbon measured values could be different for particles actually having the same numbers of carbon atoms in them. And it is possible to postulate that aerosol coatings or adsorbents, or particle morphology, could also give rise to different absorption coefficients than those one would observe for uncoated particles.

Experiences to date have shown that for an emission source such as a late model diesel that is rich in EC, the improve protocol method of quantifying EC (37) correlates

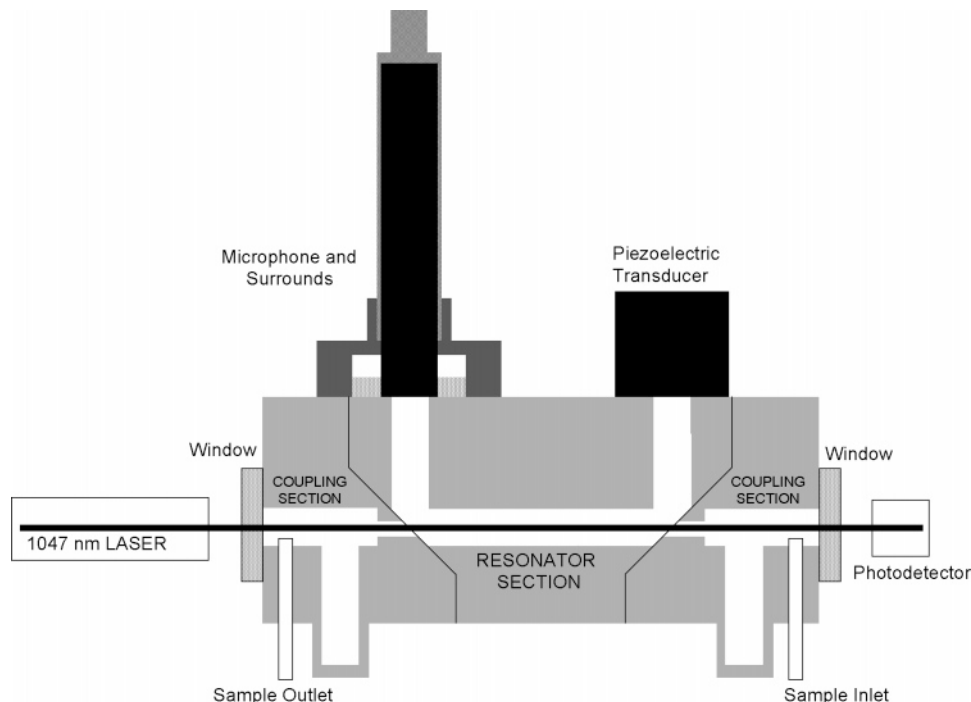


FIGURE 2. Schematic representation of the new acoustical resonator used in the photoacoustic instrument.

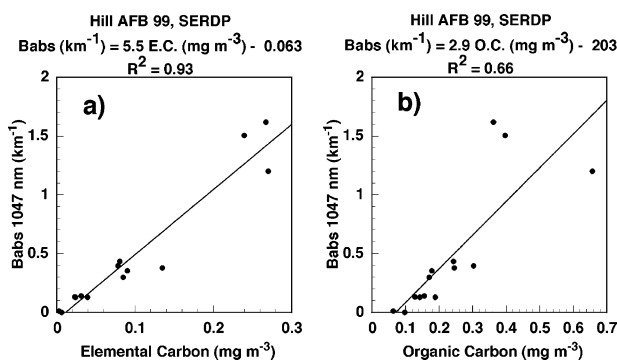


FIGURE 3. Aerosol light absorption measurements for gasoline and diesel vehicles at Hill Air Force Base. Comparison with elemental and organic carbon measurements are shown in a and b, respectively. The two left-most data points on each figure are from gasoline vehicles. Vehicles were either idling or were elevated idling and were not under any other load.

well with the aerosol light absorption measurement at 1047 nm. Figure 3 shows comparisons of aerosol light absorption at 1047 nm with EC and organic carbon (OC) from data acquired on quartz fiber filters and analyzed by the thermal optical reflectance method, improve protocol. The vehicles were operated at idle or advanced idle with no load (38). Note the good correlation of EC with BC (Figure 3a) and the relatively poor correlation of OC with BC (Figure 3b). However, the data tends to group into 4 sets, almost as 4 points. It would have been desirable to have the data densely fill a wide dynamic range of concentrations to fully evaluate the intercomparison between EC and BC measurements. The data shown in Figure 3 does not imply that improve EC is a carbon aerosol measurement standard that all other methods are to be compared against, but is shown to illustrate the relationship between improve carbon and photoacoustic BC. The offset between EC and BC measurements is negligible, but is substantial between BC and OC. The lack of offset in the EC case indicates that the photoacoustic instrument has a negligible response to the various exhaust gases. The EC to total carbon ratio ranged from 0.1 to 0.4, and yet no systematic influence was seen on the correlation

of BC with EC, addressing at least in a cursory manner the issues of particle coatings and refractive index variations.

The photoacoustic instrument used for the work at the Hill Air Force Base in 1999 was not actually the one shown schematically in Figure 2, but was a previous prototype (28) that was modified for use with the 1047-nm laser. Successful use of this prototype instrument was the impetus to develop the resonator shown schematically in Figure 2. The data from the second round of measurements at the Hill Air Force base in 2000 are described below. The data in Figure 3a gave the impetus to accept the 1047-nm laser operation as ideal, and to move forward with the improved resonator design shown in Figure 2. The prototype resonator was operated at both its fundamental acoustic frequency of 500 Hz and in exploration of the noise reduction potential at the next available harmonic at 1500 Hz, even though the resonator coupling efficiency at the higher frequency is only $1/3$ of its value at 500 Hz. A significant reduction in the effects of ambient noise were noted in the 1500-Hz operation, and so the resonator design shown in Figure 2 was made with dimensions essentially $1/3$ those of the prototype so that it operates in its fundamental mode of 1500 Hz.

From this point forward, the following relationship was used to obtain the black carbon concentration from the aerosol light absorption measurement at 1047 nm:

$$BC (\mu\text{g m}^{-3}) = \frac{B_{\text{abs}} (\text{Mm}^{-1})}{5 (\text{m}^2 \text{g}^{-1})} (\text{measured at 1047 nm}) \quad (1)$$

Most of the data in Figure 3 represents diesel emissions. EC from diesels provide a relatively unambiguous measurement from the various protocols and methods that have been developed, although ambient and wood smoke samples have substantial differences (39, 40). For these reasons, it is good to use diesel emissions as a starting point to establish essentially an EC standard and to use the BC measurement by the photoacoustic method as a standard for other types of sources.

BC and EC measurements for gasoline and diesel vehicles used in ground support at Hill Air Force Base were obtained in 2000 (41) and are shown in Figure 4. However, the data

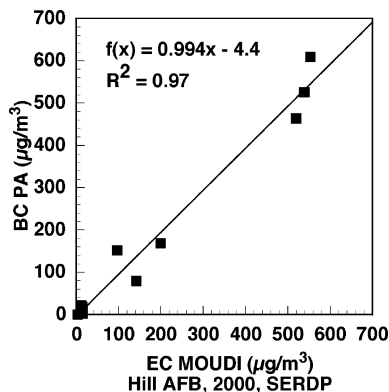


FIGURE 4. Black carbon and elemental carbon measurements for gasoline and diesel vehicles operated under load. The gasoline vehicles were particularly clean and provided the left-most data points. These measurements were made using the photoacoustic instrument shown schematically in Figure 2.

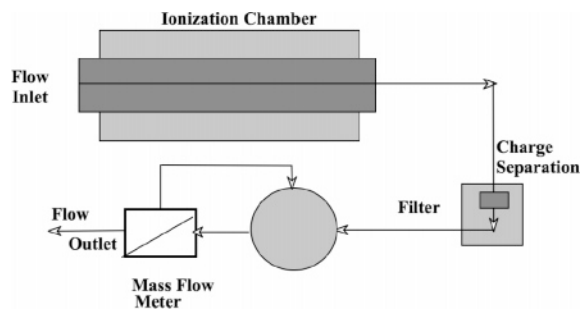


FIGURE 5. Schematic of the photoelectric aerosol sensor (PAS).

tends to group into 3 sets, almost as 3 points. It would have been desirable to have the data densely fill a wide dynamic range of concentrations to fully evaluate the intercomparison between EC and BC measurements. The EC fraction ranged from 2.5 to 35% of the total carbon in these measurements, and the vehicle engine load ranged from idle to 93%. The photoacoustic instrument used in these measurements is the one shown schematically in Figure 2. This time the EC measurements were made on the aluminum foil substrates used in a MOUDI sampler. TOR analysis for these substrates simply skips the pyrolysis correction stage and moves directly from OC4 to EC1. Most EC from diesel sources is contained in the EC2 phase (40), so the pyrolysis correction is not so important to the data shown in Figure 4. It should be noted that the EC from MOUDI analysis correlated well with that obtained by the quartz filter analysis for the data shown in Figure 3; however, the quartz filter sampler had a leak in the 2000 SERDP experiment.

Photoelectric Aerosol Sensor. The photoelectric aerosol sensor 2000 (PAS2000 EcoChem Messtechnik GmbH) qualitatively measures the concentration of particle-bound polycyclic aromatic hydrocarbons (pPAHs). Figure 5 shows a schematic of the PAS, and additional instrument details can be found in refs 16, 42, and 43. Briefly, the PAS uses a KrCl excimer lamp operating at 222 nm as a photoionization source; the photon energy of the lamp is chosen so that gas-phase molecules are negligibly ionized. Samples flow continuously into the excimer-lamp ionization region, where particle-bound PAH molecules are ionized and lose an electron. The positively charged particles collect on a filter where charge is measured with an electrometer. The charge is integrated over time to give the photoelectric current (in femto- or picoamps), and this current should be proportional to the PAH loading on particles.

Particles that are very porous may have regions where deposited PAHs cannot contribute to the photoelectric

current (44). The photoelectric yield depends on the type of particles, such as sodium chloride, aluminum oxide, or carbon, that the PAH has been adsorbed upon (44). It is recognized that a meaningful interpretation of the photoelectric signal can be obtained only when the relative abundance of the various PAHs adsorbed on particles are constant, because different PAHs have very different influences on photoemission (42). Because photoemission is a surface technique, the linearity of photoelectric yield with the PAH amount can only be expected for monolayers of PAH adsorbed on particles, and any other substance adsorbed on top of the PAHs will likely quench photoemission (43). Photoelectric signals have been observed for uncoated black carbon particles (44, 45). In summary, although the PAS instrument has a sensitivity for 1 s of integration time of around 1 ng m^{-3} PAH concentration (43), a great number of circumstances can influence the linearity of photoelectric yield with PAH type and concentration. It is the purpose of this paper to explore the photoelectric yield in practice for samples obtained directly from a variety of combustion sources.

Successful use of the PAS instrument for source-samples required operation with a heated inlet as described in more detail in the following section. Aerosol photoemission per unit particle surface area (APE) has been measured as a function of temperature for spark and compression ignition engines (SI and CI, respectively) and for an oil burner (46). A thermal desorption unit operating in the temperature range from ambient to 325 °C was used to remove volatile material from combustion aerosol to quantify the effects of temperature on APE. A substantial increase of APE was observed for exhaust from CI and SI engines when the temperature reaches 125 to 200 °C, respectively. The particle diameter was reduced substantially for the CI and SI engines under low load because the relative fraction of semivolatiles on these particles is high under low load, but they go to the gas phase as the temperature increases. However, for the diesel CI engine under high load, as well as for the oil burner operated in an air-starved rich fuel condition, most of the particulate matter is BC, and the change of particle diameter with temperature is small. APE increased with temperature initially for the high-load CI case, but remained constant across a large temperature range where the particle size was constant. For rich operation of the oil burner, APE was essentially constant up to a temperature of 350 °C. The gas-to-particle phase partition for particle-bound PAHs would increasingly favor progressively higher molecular weight PAHs in the gaseous state as the temperature increases. One might expect to see a diminishment of APE with temperature as more PAHs go into the gas state, especially when only a monolayer of PAH is left on the particles. However this was not observed. One interpretation of this work is that the observed APE at high temperature could be coming from the polycyclic nature of the black carbon particle alone even if all of the particle-bound PAH has been desorbed. This interpretation seems consistent with the lack of gradual change of APE with increasing temperature for the high load cases and for the leveling out of APE for the low loaded cases when semivolatile material is removed from the particle surface to expose the underlying black carbon.

Relationship of Photoelectric Yield and Black Carbon Concentration from Gasoline and Diesel Powered Vehicles and Jet Aircraft Exhaust. During the course of this study, temperature and exhaust concentration were identified as important factors governing the response and reproducibility of PAS readings. For sampling exhaust from vehicles or aircraft, a PAS inlet temperature of at least 120 °C produced more stable results than lower inlet temperatures. Even with dilution, it is possible that vehicles and aircraft contain enough vapor-phase hydrocarbons and water vapor in their

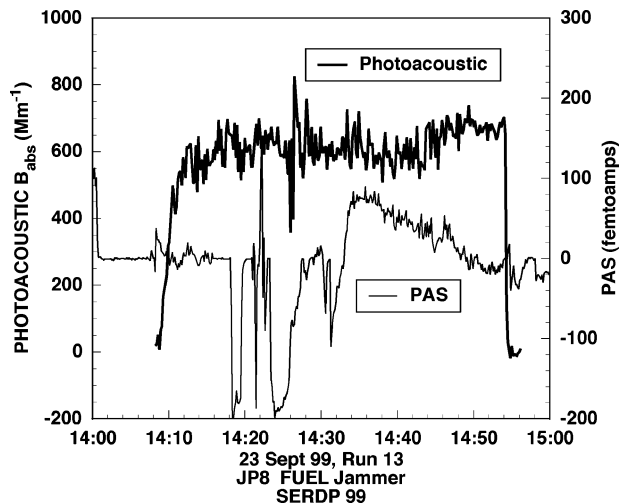


FIGURE 6. Time series showing aerosol light absorption on the left axis and photoelectric aerosol sensor current on the right axis, for a “Jammer” vehicle operated on JP8 fuel. Note the substantial periods when the PAS signal is negative, and the perhaps unexpected decay of the PAS signal around time 14:40. This is a typical series for the PAS before the instrument was thoroughly cleaned and before the PAS inlet was heated to 150 °C.

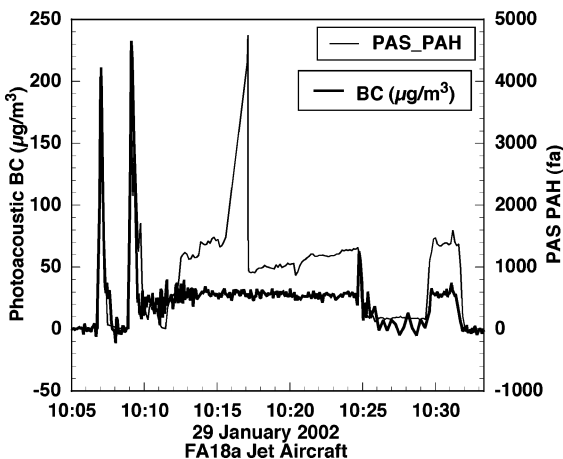


FIGURE 7. Time series for photoacoustic black carbon and photoelectric aerosol sensor measurements from a tethered FA18a jet aircraft under variable load. Curves nearly overlap after crank-up, between 10:05 and 10:10. The time interval 10:25–10:30 had the greatest load (80% full power) and lowest emission concentrations because the aircraft was pulling in more dilution air at this time. Data are from SERDP 2002.

exhaust to condense inside the PAS and produce erratic results, as illustrated for example in Figure 6 data from the 1999 SERDP project (38). In addition, exposing the PAS directly to undiluted exhaust caused spurious negative signals. The PAS inlet was heated to a constant temperature of 150 °C to maintain stable PAS readings during this study; the exhaust was diluted with dry, particle-free air; and the PAS response was generally maintained in the femtoamp range.

Figure 7 shows the time series of emissions from a FA18a jet aircraft obtained with the PAS and PA. The aircraft was in for repairs at the Navy base on North Island, San Diego, CA, and an eductor system was used to dilute the exhaust with a dilution ratio of about 1:15. The aircraft was brought from idle to 80% of full power. Exhaust emissions become more diluted by ambient air as the aircraft power setting increases. Note that the PAS curve is positive everywhere, and at times, matches the form of the BC curve. In general, it is not expected that the PAS and BC curves should be in

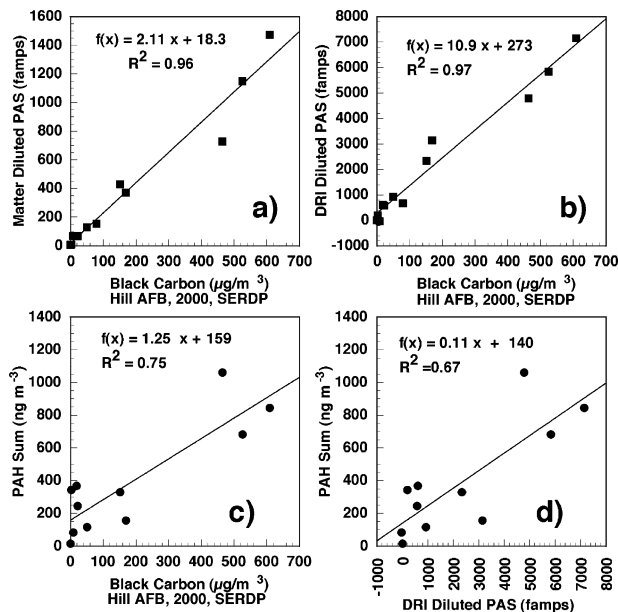


FIGURE 8. Scatter plot of black carbon and PAS measurements of emissions from gasoline and diesel vehicles during SERDP 2000. In part a, PAS sampled behind the so-called Matter dilution system, and in part b, a second PAS sampled behind the DRI dilution tunnel. In both cases, the BC measurements were obtained behind the DRI dilution tunnel. Note the high degree of correlation of PAS and BC data. Extractive PAHs are shown in c and d against BC and the PAS. Linear regressions in c and d are subject to substantial data clumping around the lowest and highest values and to the uncertainty in the PAH measurements. Particle-bound PAH blanks were around 30 ng m⁻³ and can be viewed as one measure of the uncertainty in the PAH measurement.

1:1 correspondence because the PAH emission rate may be different from that of the BC. Also note that Figure 7 shows that the photoacoustic instrument can provide useful data even in a very loud environment.

Figure 8 shows measurements of emissions from gasoline and diesel vehicles from SERDP 2000 (41). It would have been desirable to have the data densely fill a wide dynamic range of concentrations to fully evaluate the intercomparison between PAS, PAH, and BC measurements because the data tends to clump into groups. Two PAS instruments were used, with one behind the DRI dilution system (described in ref 38) and one behind the so-called Matter dilution system (47). The Matter dilution system samples directly from the tailpipe. Note that in both cases, Figure 8a and b, the correlation of PAS signals with BC measurements is quite high, perhaps suggesting that PAH production is correlated highly with BC production and/or that the PAS responds directly to BC. It could also be that the need to operate the PAS with an inlet at 150 °C favors PAHs being in the vapor phase. The 14 PAH compounds used in the PAH sum are: phenanthrene, fluoranthene, pyrene, benzo[*b*]naphtho(2,1-*d*)thiophene, benzo(ghi)fluoranthene, benzo[*c*]phenanthrene, benz[*a*]anthracene, chrysene, triphenylene, benzo(1,2,3-*cd*)fluoroanthene, benzo[*e*]pyrene, indeno(1,2,3-*cd*)pyrene, benzo(ghi)perylene, and coronene. The sum has also been used by others seeking relationships between photoelectric yield and PAHs (48). At 150 °C, fluoranthene and pyrene are going to be nearly exclusively in the gas phase, and benzo[*b*]naphtho(2,1-*d*)thiophene, benzo(ghi)fluoranthene, benzo[*c*]phenanthrene, benz[*a*]anthracene, and chrysene/triphenylene substantially partitioned to the gas phase. The gas/particle distribution determined using a denuder system at room temperature does not correspond to this distribution at 150 °C.

However, extractive measurements of PAHs do not show a strong correlation of black carbon with the ratio of particle

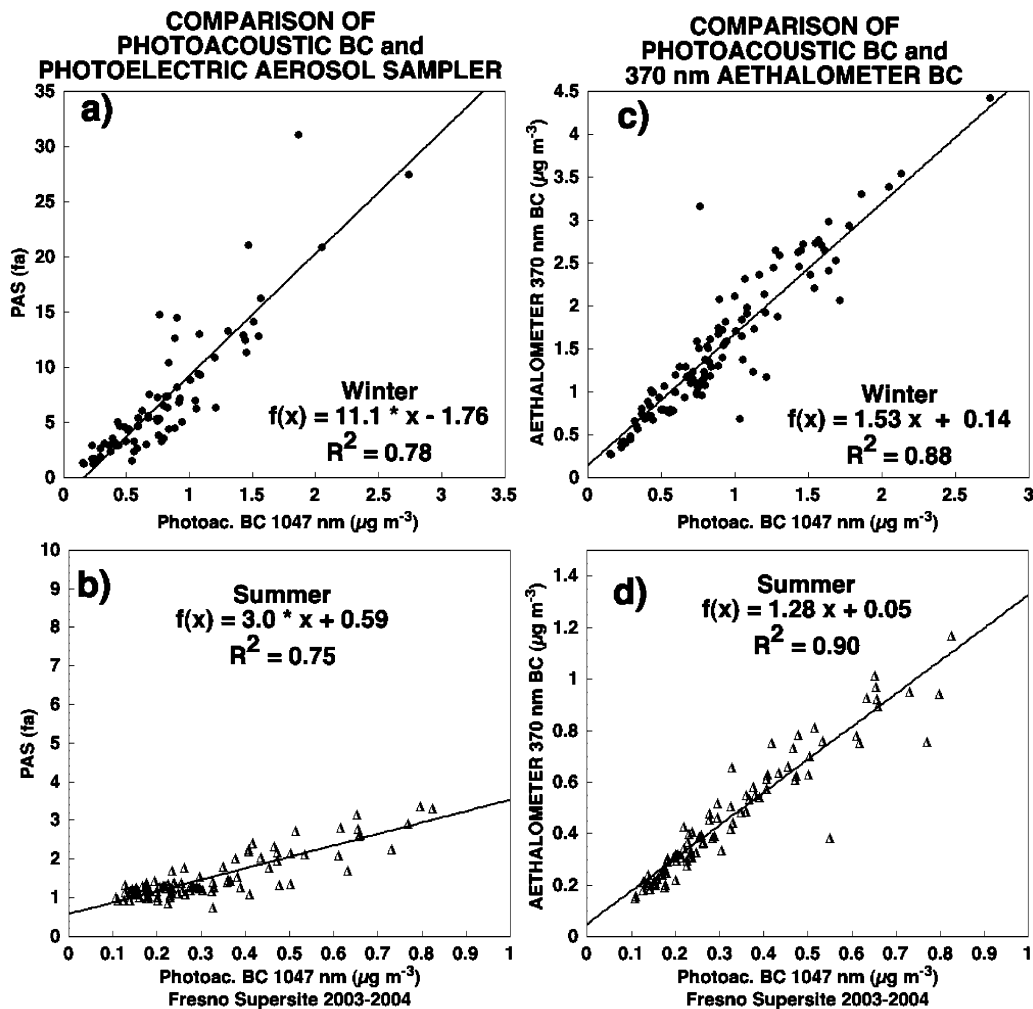


FIGURE 9. Comparison of daily averaged photoacoustic BC measurements at 1047 nm with a and b photoelectric aerosol sampler data and with c and d aethalometer BC measurements at 370 nm. Correlations with winter data are shown in a and c, and summer data in b and d. Open triangles are summer data, solid circles are winter data. The scales of the axes in a and c are a factor of 3 larger than those of b and d because winter concentrations are about a factor of 3 larger than summer conditions. Winter data are for December 1 through March 30 and summer data are for April 1 through June 30.

to gas phase concentrations of pyrene and fluoranthene for the vehicles whose emission is reported in Figure 8 (5). The sum of particle-bound PAHs are shown in Figure 8c and d against BC and the PAS, respectively. Note in Figure 8c that the data tends to clump into two super data points, and the wide spread of values at the low end, likely due to the uncertainty in the PAH measurement as well as due to the variations of emissions from different sources. The substantial offset is perhaps suggestive that the particle-bound PAHs are not exclusively associated with BC. Note that the slope of the linear curve fit implies around 1.25 ng of particle-bound PAH produced per 1 ug of BC. A ratio of around 1 (and for gasoline vehicles, 3) ng particle-bound PAH per ug BC can be calculated from the tunnel study data reported in ref 49.

The PAS versus extractive PAH measurements are shown in Figure 8d. The data clumping is not as severe as that in Figure 8c, and the correlation is modest. The slope of the curve, 0.11 ng m⁻³/femtoamp, is consistent with the values found in an ambient study in Italy where traffic and meteorological inversions contributed to the observed levels of air pollutants. Some fraction of the pPAH is adsorbed into the organic carbon particulate in the exhaust, particularly the lower molecular weight higher vapor pressure molecules; not all of the pPAH is adsorbed to the surface of elemental carbon aerosol (50). Much of the organic carbon fraction

may be volatilized by the use of the 150 °C inlet on the PAS necessary to avoid negative signals such as those shown in Figure 6. These negative signals may be due to charge separation occurring during the evaporation of relatively volatile aerosol from the PAS filter, similar to happens with water droplets in the atmosphere (51). PPAHs adsorbed or absorbed in a film thicker than a single molecular level would very likely have their charge separation from the UV lamp quenched so as not to contribute to the PAS signal anyway (43). From the good correlation of PAS and BC measurements as shown in Figure 8a and b, it is to be concluded that the PAS responds to pPAHs that are produced in combustion at the same rate as BC, or more likely, that a good portion of the PAS response can be due to the BC itself.

Relationship of Photoelectric Yield and Black Carbon Concentration for Ambient Air. The purpose of this section is to contrast the PAS and PA comparison from source samples as discussed above with a comparison of ambient data measurements. The heated inlet is generally not needed to operate the PAS for ambient samples because the concentrations are generally lower as are the effects of condensation and evaporation of semivolatile material. A PAS instrument was collocated with a PA at the Fresno Supersite in Fresno, CA from December 2003 through July 2004 to sample ambient air in association with the Environmental Protection Agency's Supersite Study Program. Fresno is an interesting location

for aerosol instrumentation characterization because two distinct seasonal conditions are commonly observed (52). Winter conditions in Fresno are stagnant with long periods of fog and air pollution from wood burning for residential heat, vehicle use, and resuspended road dust. Summer conditions are dry and much less stagnant. Wood-burning activity is uncommon, although agricultural practices are more active in the general Central Valley region. Aerosol aging is much more significant in the winter than in the summer, and the cooler temperatures are associated with more condensation of vapors onto particle surfaces. Vehicles are likely to have higher PM emission rates in winter than in summer.

Indeed, the Fresno data shown in Figure 9a–d naturally segregated into two groups, labeled winter and summer. The winter data group spans from the beginning of December until the end of March, and the summer group spans from the first of April until the end of June. The photoacoustic instrument was operated during both seasons with no operator intervention or adjustment of any kind. Both two and seven wavelength aethalometers were also operated in Fresno during this time. The aethalometer (53) is a filter-based instrument that is used to measure aerosol BC by measuring aerosol light absorption, much in analogy to the way BC is measured by the photoacoustic method. The filter-based method is simpler to implement than the photoacoustic method, although the conversion of optical attenuation by a filter with embedded aerosol to an in-situ aerosol light absorption coefficient is less straightforward than it is for the photoacoustic method because of the loading-dependent filter-multiple-scattering-enhancement of aerosol light absorption and an offset due to light backscattered by particles on the filter (13). The near-IR channels at 880 and 950 nm of the aethalometer respond mainly to the quasi-graphitic strongly light-absorbing aerosol (i.e., BC). However, the 370-nm UV channel of the aethalometer also responds to strongly absorbing organic compounds such as PAHs that may also be present on particles. The aethalometer manufacturer is careful to point out that this UV channel is not a quantitative measure of particle-bound PAH because different compounds have different mass absorption efficiencies for aerosol light absorption (see <http://www.mageesci.com> for more details). When the UV channel BC measurement is in excess of the near-IR channel, it is said that organic light-absorbing compounds are present and that these compounds are likely PAHs.

Figure 9a and b shows that the winter conditions have 3.7 times as much PAS signal (i.e., pPAH) per unit photoacoustic BC than the summer conditions. Figure 9c and d shows that the UV 370-nm channel of the aethalometer is higher in winter than it is in summer. Both of these observations are compatible with the meteorological conditions and emission sources observed in these seasons. The correlation of the aethalometer and photoacoustic BC data is high and the offset, although small, is nonzero, perhaps indicating that the aethalometer responds to something that the photoacoustic instrument does not respond to, such as the aerosol backscattering coefficient. The aethalometer data has not been corrected for scattering aerosol offset or for filter-loading effects, although the latter effect would tend to increase the winter slope while having a modest effect on the summer slope (13). These ambient measurements illustrate that the PAS instrument responds to more than the BC measurement made at 1047 nm in conditions, such as winter in Fresno, when a heated inlet is not used with the PAS.

Discussion

The goal at the outset of this work was to evaluate the PAS calibration for measurement of pPAH by comparing the time-integrated values with the corresponding laboratory analysis

of a sum of PAHs obtained through use of a denuder-filter-based system. Real-time BC measurements were similarly evaluated against filter-based EC measurements by the IMPROVE protocol. BC provides a primary surface for adsorption of pPAH. Combustion processes are likely to produce both pPAH and BC, so it is perhaps expected to find a correlation between BC and PAS measurements.

Operational difficulties were encountered when the PAS was used to sample from combustion sources such as spark and compression ignition vehicles. Spurious negative signals were observed until the inlet air was heated to around 150 °C, although at the expense of upsetting the gas-to-particle phase partition. The PAH sum shown in Figure 8c and d had modest correlation with BC and PAS measurements. The PAS and BC measurement for source-samples had a high degree of correlation as shown in Figure 8a and d, raising the question that the PAS perhaps responds to BC in addition to pPAH. The BC measurements at 1047 nm are not affected by light absorption due to pPAH because they absorb predominantly at UV wavelengths.

The PAS was also employed to measure ambient air without the use of a heated inlet. This time the correlation of PAS and BC measurements was modest as shown in Figure 9a and b. A distinct seasonal difference was observed between PAS and BC measurements.

Taken together, the ambient and source measurements suggest that the PAS may respond to BC in addition to pPAH. Some fraction of the BC surface, within a thin boundary layer, may give rise directly to APE. The mass concentration of pPAH is roughly one thousandth that of BC, although a monolayer of pPAH could cover a substantial portion of the BC surface. It is possible that use of the heated inlet left only heavier molecular weight PAHs in the particle phase and that these PAHs are produced in concert with BC during combustion. The PAS appears to produce only a qualitative measure of pPAH.

Acknowledgments

This research was supported by the Strategic Environmental Research and Development Program, Project CP-1106. We thank Bob Armstrong of HAFB for his assistance with the vehicles and John Walker of DRI for assistance with aspects of the photoacoustic instrument design. James B. Griffin, Jacob D. McDonald, and Dana Overacker contributed to the conduct of the first SERDP experiment in 1999 and thus to the laying of the groundwork for what was to follow in subsequent experiments. This study was also cosponsored by the U.S. Environmental Protection Agency (EPA) under contract no. R-82805701 for the Fresno Supersite and under the EPA STAR grant RD-83108601-0. We acknowledge sponsorship of the National Science Foundation for instrument development.

Literature Cited

- 1) Andreae, M. O. The dark side of aerosols. *Nature* **2001**, *409*, 671–672.
- 2) Lighty, J. S.; Veranth, J. M.; Sarofim, A. F. Combustion aerosols: Factors governing their size and composition and implications to human health. *J. Air Waste Manage. Assoc.* **2001**, *50*, 1565–1618.
- 3) Ramanathan, V.; Crutzen, P. J. New Directions: Atmospheric Brown “Clouds”. *Atmos. Environ.* **2003**, *37*, 4033–4035.
- 4) Novakov, T.; Ramanathan, V.; Hansen, J. E.; Kirchstetter, T. W.; Sato, M.; Sinton, J. E.; Sathaye, J. A. Large historical changes of fossil-fuel black carbon aerosols. *Geophys. Res. Lett.* **2003**, *30*, doi: 10.1029/2002GL016345.
- 5) Zielinska, B.; Sagebiel, J.; Arnott, W. P.; Rogers, C. F.; Kelly, K. E.; Wagner, D. A.; Lighty, J. S.; Sarofim, A. F.; Palmer, G. Phase and size distribution of polycyclic aromatic hydrocarbons in diesel and gasoline vehicle emissions. *Environ. Sci. Technol.* **2004**, *38*, 2557–2567.

- (6) Mader, B. T.; Pankow, J. F. Study of the effects of particle-phase carbon on the gas/particle partitioning of semivolatile organic compounds in the atmosphere using controlled field experiments. *Environ. Sci. Technol.* **2002**, *36*, 11.
- (7) Naumova, Y. Y.; Eisenreich, S. J.; Turpin, B. J.; Weisel, C. P.; Morandi, M. T.; Colome, S. D.; Totten, L. A.; Stock, T. H.; Winer, A. M.; Alimokhtari, S.; Kwon, J.; Shendell, D.; Jones, J.; Maberti, S.; Wall, S. J. Polycyclic aromatic hydrocarbons in the indoor and outdoor air of three cities in the U.S. *Environ. Sci. Technol.* **2002**, *36*, 8.
- (8) Naumova, Y. Y.; Offenberg, J. H.; Eisenreich, S. J.; Meng, Q.; Polidori, A.; Turpin, B. J.; Weisel, C. P.; Morandi, M. T.; Colome, S. D.; Stock, T. H.; Winer, A. M.; Alimokhtari, S.; Kwon, J.; Maberti, S.; Shendell, D.; Jones, J.; Farrar, C. Gas/particle distribution of polycyclic aromatic hydrocarbons in coupled outdoor/indoor atmospheres. *Atmos. Environ.* **2003**, *37*, 18.
- (9) Pankow, J. F. Gas/particle partitioning of neutral and ionizing compounds to single and multiphase aerosol particles I Unified modeling framework. *Atmos. Environ.* **2003**, *37*, 12.
- (10) NTP 10th Report on Carcinogen; National Toxicology Program. U.S. Department of Health and Human Services, National Toxicology Program, 2003.
- (11) IARC, International Agency for Research on Cancer, 2003.
- (12) Nel, A. E.; Diaz-Sanchez, D.; Ng, D.; Hiura, T.; Saxon, A. Updates on cells and cytokines – Enhancement of allergic inflammation by the interaction between diesel exhaust particles and the immune system. *J. Allergy Clin. Immunol.* **1998**, *102*, 539–554.
- (13) Arnott, W. P.; Hamasha, K.; Moosmüller, H.; Sheridan, P. J.; Ogren, J. A. Towards aerosol light absorption measurements with a 7-wavelength Aethalometer: Evaluation with a photoacoustic instrument and a 3 wavelength nephelometer. *Aerosol Sci. Technol.* **2005**, *39*, 17–29.
- (14) Horvath, H. Systematic deviations of light absorption measurements by filter transmission methods. *J. Aerosol Sci.* **1997**, *28*, S55–S56.
- (15) Sheridan, P. J.; Arnott, W. P.; Ogren, J. A.; Anderson, B. E.; Atkinson, D. B.; Covert, D. S.; Moosmüller, H.; Petzold, A.; Schmid, B.; Strawa, A. W.; Varma, R.; Virkkula, A. The Reno aerosol optics study: An Evaluation of Aerosol Absorption Measurement Methods. *Aerosol Sci. Technol.* **2005**, *39*, 1–16.
- (16) EPA Field and Laboratory Analyses of a Real-Time PAH Analyzer; EPA/600/R-97/034; EPA Office of Research and Development, 1997.
- (17) Wilson, N. K.; Barbour, R. K. Evaluation of a real-time monitor for fine particle-bound PAH in air, Polycyclic Aromatic Compound. *Polycyclic Aromat. Compd.* **1994**, *5*, 167–174.
- (18) Wilson, N. K.; Chuang, J. C. Sampling polycyclic aromatic hydrocarbons and related semivolatile organic compounds in indoor air. *Indoor Air* **1991**, *4*, 512–513.
- (19) Agnesod, G.; Maria, R. D.; Fontana, M.; Zublena, M. Determination of PAH in airborne particulate: Comparison between off-line sampling techniques and an automatic analyser based on a photoelectric aerosol sensor. *Sci. Total Environ.* **1996**, *189–190*, 443–449.
- (20) Chetwittayachan, T.; Shimazaki, D.; Yamamoto, K. A comparison of temporal variation of particle-bound polycyclic aromatic hydrocarbons (pPAHs) concentration in different urban environments: Tokyo, Japan, and Bangkok, Thailand. *Atmos. Environ.* **2002**, *36*, 2027–2037.
- (21) Chuang, J. C.; Callahan, P. J.; Lyu, C. W.; Wilson, N. K. Polycyclic aromatic hydrocarbon exposures of children in low-income families. *J. Exposure Anal. Environ. Epidemiol.* **1999**, *2*, 85–98.
- (22) Roessler, D. M. Photoacoustic insights on diesel exhaust particles. *Appl. Opt.* **1984**, *23*, 1148–1155.
- (23) Japar, S. M.; Killinger, D. K. Photoacoustic and absorption spectrum of airborne carbon particulate using a tunable dye laser. *Chem. Phys. Lett.* **1979**, *66*, 207–209.
- (24) Japar, S. M.; Szkarlat, A. C. Measurement of diesel vehicle exhaust particulate using photoacoustic spectroscopy. *Combust. Sci. Technol.* **1981**, *24*, 215–219.
- (25) Terhune, R. W.; Anderson, J. E. Spectrophone measurements of the absorption of visible light by aerosols in the atmosphere. *Opt. Lett.* **1977**, *1*, 70–72.
- (26) Japar, S. M.; Szkarlat, A. C. In Real-time measurements of diesel vehicle exhaust particulate using photoacoustic spectroscopy and total light extinction, Fuels and Lubricants Meeting, Tulsa OK, 1981; SAE: Tulsa OK, 1981; pp 1–8.
- (27) Japar, S. M.; Szkarlat, A. C.; Pierson, W. R. The determination of the optical properties of airborne particle emissions from diesel vehicles. *Sci. Total Environ.* **1984**, *36*, 121–130.
- (28) Arnott, W. P.; Moosmüller, H.; Rogers, C. F.; Jin, T.; Bruch, R. Photoacoustic spectrometer for measuring light absorption by aerosols: Instrument description. *Atmos. Environ.* **1999**, *33*, 2845–2852.
- (29) Moosmüller, H.; Arnott, W. P.; Rogers, C. F.; Bowen, J. L.; Gillies, J. A.; Pierson, W. R.; Collins, J. F.; Durbin, T. D.; Norbeck, J. M. Time-resolved characterization of particulate emission: 2. Instruments for elemental and organic carbon measurements. *Environ. Sci. Technol.* **2001**, *35*, 1935–1942.
- (30) Petzold, A.; Niessner, R. In The Photoacoustic Soot Sensor for Black Carbon Monitoring, Fifth International Conference on Carbonaceous Particles in the Atmosphere, Berkeley, CA, 1994; p 72.
- (31) Petzold, A.; Niessner, R. Novel design of a resonant photoacoustic spectrophone for elemental carbon mass monitoring. *Appl. Phys. Lett.* **1995**, *66*, 1285–1287.
- (32) Adams, K. M.; Japar, S. M.; Pierson, W. R. Development of a MnO₂-coated, cylindrical denuder for removing NO₂ from atmospheric samples. *Atmos. Environ.* **1986**, *20*, 1211–1215.
- (33) Arnott, W. P.; Moosmüller, H.; Walker, J. W. Nitrogen dioxide and kerosene-flame soot calibration of photoacoustic instruments for measurement of light absorption by aerosols. *Rev. Sci. Instrum.* **2000**, *71*, 4545–4552.
- (34) Arnott, W. P.; Moosmüller, H.; Walker, J. W. Photoacoustic instrument for measuring particles in a gas. U.S. Patent 6,662,627, December 16, 2003.
- (35) Dalzell, W. H.; Sarofim, A. F. Optical constants of soot and their application to heat flux calculations. *J. Heat Transfer* **1969**, *100–104*.
- (36) Fuller, K. A.; Malm, W. C.; Kreidenweis, S. M. Effects of mixing on extinction by carbonaceous particles. *J. Geophys. Res.* **1999**, *104*, 15941–15954.
- (37) Chow, J. C.; Watson, J. G.; Pritchett, L. C.; Pierson, W. R.; Frazier, C. A.; Purcell, R. G. The DRI thermal/optical reflectance carbon analysis system: Description, evaluation and applications in U.S. air quality studies. *Atmos. Environ.* **1993**, *27A*, 1185–1201.
- (38) Rogers, C. F.; Sagebiel, J. C.; Zielinska, B.; Arnott, W. P.; Fujita, E. M.; McDonald, J. D.; Griffin, J. B.; Kelly, K.; Overacker, D.; Wagner, D.; Lighty, J. S.; Sarofim, A.; Palmer, G. Characterization of submicron exhaust particles from engines operating without load on diesel and JP-8 fuels. *Aerosol Sci. Technol.* **2003**, *37*, 355–368.
- (39) Chow, J.; Watson, J.; Crow, D.; Lowenthal, D.; Merrifield, T. Comparison of IMPROVE and NIOSH carbon measurements. *Aerosol Sci. Technol.* **2001**, *34*, 23–34.
- (40) Watson, J. G.; Chow, J. C.; Lowenthal, D. H.; Pritchett, L. C. Differences in the carbon composition of source profiles for diesel- and gasoline-powered vehicles. *Atmos. Environ.* **1994**, *28*, 2493–2505.
- (41) Kelly, K. E.; Wagner, D. A.; Lighty, J. S.; Sarofim, A. F.; Rogers, C. F.; Sagebiel, J.; Zielinska, B.; Arnott, W. P.; Palmer, G. Characterization of exhaust particles from military vehicles fueled with diesel, gasoline, and JP-8. *J. Air Waste Manage. Assoc.* **2003**, *53*, 273–282.
- (42) Burtscher, H. Measurement and characteristics of combustion aerosols with special consideration of photoelectric charging and charging by flame ions. *J. Aerosol Sci.* **1992**, *23*, 549–595.
- (43) Burtscher, H.; Siegmann, H. C. Monitoring PAH-emissions from combustion processes by photoelectric charging. *Combust. Sci. Technol.* **1994**, *101*, 327–332.
- (44) Niessner, R.; Wilbring, P. Ultrafine particles as trace catchers for polycyclic aromatic hydrocarbons: The photoelectric aerosol sensor as a tool for in situ sorption and desorption studies. *Anal. Chem.* **1989**, *61*, 708–714.
- (45) Baltensperger, U. E.; Weingartner, H.; Burtscher, J.; Keskiö, J. Dynamic mass and surface area measurements. In *Aerosol Measurement*; Baron, P. A., Willeke, K., Eds.; Wiley: New York, 2001; pp 387–418.
- (46) Steiner, D.; Burtscher, H. Studies on the dynamics of adsorption and desorption from combustion particles, by temperature-dependent measurement of size, mass, and photoelectric yield. *Water, Air, Soil Pollut.* **1993**, *68*, 159–176.
- (47) Hueglin, C.; Scherrer, L.; Burtscher, H. An accurate, continuously adjustable dilution system (1:10 to 1:10⁴) for submicron aerosols. *J. Aerosol Sci.* **1997**, *28*, 1049–1055.
- (48) McDow, S.; Giger, W.; Burtscher, H.; Schmidt-ott, A.; Siegmann, H. C. Polycyclic aromatic hydrocarbons and combustion aerosol photoemission. *Atmos. Environ.* **1990**, *24*, 2911–2916.
- (49) Miguel, A. H.; Kirchstetter, T. W.; Harley, R. A.; Hering, S. V. On-road emissions of particulate polycyclic aromatic hydrocarbons and black carbon from gasoline and diesel vehicles. *Environ. Sci. Technol.* **1998**, *32*, 6.

- (50) Allen, J. O.; Sarofim, A. F.; Smith, K. A. A critical evaluation of two proposed atmospheric partitioning mechanisms, adsorption and absorption, using atmospheric data for polycyclic aromatic hydrocarbons. *J. Aerosol Sci.* **1997**, *28*, S335–S336.
- (51) Dong, Y.; Hallett, J. Charge separation by ice and water drops during growth and evaporation. *J. Geophys. Res.* **1992**, *97*, (D18), 20,361.
- (52) Lawless, P. A.; Rodes, C. E.; Evans, G.; Sheldon, L.; Creason, J. Aerosol concentrations during the 1999 Fresno exposure studies as functions of size, season, and meteorology. *Aerosol Sci. Technol.* **2001**, *34*, 66–74.
- (53) Hansen, A. D. A.; Rosen, H.; Novakov, T. The aethalometer – An instrument for the real-time measurement of optical absorption by aerosol particles. *Sci. Total Environ.* **1984**, *36*, 191–196.

Received for review March 15, 2004. Revised manuscript received April 5, 2005. Accepted April 29, 2005.

ES049595E